



# Investigation of Teflon FEP Embrittlement on Spacecraft in Low Earth Orbit

Kim K. de Groh  
Lewis Research Center, Cleveland, Ohio

Daniela C. Smith  
Cleveland State University, Cleveland, Ohio

Prepared for the  
Seventh International Symposium on Materials in a Space Environment  
cosponsored by ONERA, CERT, CNES, and ESA/ESTEC  
Toulouse, France, June 16–20, 1997

National Aeronautics and  
Space Administration

Lewis Research Center

Trade names or manufacturers' names are used in this report for identification only. This usage does not constitute an official endorsement, either expressed or implied, by the National Aeronautics and Space Administration.

Available from

NASA Center for Aerospace Information  
800 Elkridge Landing Road  
Linthicum Heights, MD 21090-2934  
Price Code: A03

National Technical Information Service  
5287 Port Royal Road  
Springfield, VA 22100  
Price Code: A03

# INVESTIGATION OF TEFLON FEP EMBRITTLEMENT ON SPACECRAFT IN LOW EARTH ORBIT

Kim K. de Groh  
NASA Lewis Research Center  
21000 Brookpark Road, M.S. 309-2  
Cleveland, Ohio 44135  
phone: (216) 433-2297, fax: (216) 433-2221, e-mail: Kim.K.deGroh@lerc.nasa.gov

Daniela C. Smith  
Cleveland State University  
1983 E. 24th Street  
Cleveland, Ohio 44115  
phone: (216) 687-3505, fax: (216) 523-7200, e-mail: D.C.Smith15@popmail.csuohio.edu

## ABSTRACT

Teflon<sup>®</sup> FEP (fluorinated ethylene-propylene) is commonly used on exterior spacecraft surfaces in the low Earth orbit (LEO) environment for thermal control. Silverized or aluminized FEP is used for the outer layer of thermal control blankets because of its low solar absorptance and high thermal emittance. FEP is also preferred over other spacecraft polymers because of its relatively high resistance to atomic oxygen erosion. Because of its low atomic oxygen erosion yield, FEP has not been protected in the space environment. Recent, long term space exposures such as on the Long Duration Exposure Facility (LDEF, 5.8 years in space), and the Hubble Space Telescope (HST, after 3.6 years in space) have provided evidence of LEO environmental degradation of FEP. These exposures provide unique opportunities for studying environmental degradation because of the long durations and the different conditions (such as differences in altitude) of the exposures. Samples of FEP from LDEF and from HST (retrieved during its first servicing mission) have been evaluated for solar induced embrittlement and for synergistic effects of solar degradation and atomic oxygen. Micro-indenter results indicate that the surface hardness increased as the ratio of atomic oxygen fluence to solar fluence decreased for the LDEF samples. FEP multilayer insulation (MLI) retrieved from HST provided evidence of severe embrittlement on solar facing surfaces. Micro-indenter measurements indicated higher surface hardness values for these samples than LDEF samples, but the solar exposures were higher. Cracks induced during bend testing were significantly deeper for the HST samples with the highest solar exposure than for LDEF samples with similar atomic oxygen fluence to solar fluence ratios. If solar fluences are compared, the LDEF samples appear as damaged as HST samples, except that HST had deeper induced cracks. The results illustrate difficulties in comparing LEO exposed materials from different missions. Because the HST FEP appears more damaged than LDEF FEP based on depth of embrittlement, other causes for FEP embrittlement in addition to atomic oxygen and ultraviolet (UV) radiation, such as thermal effects and the possible role of soft x-ray radiation, need to be considered. FEP that was exposed to soft x-rays in a ground test facility, showed embrittlement similar to that witnessed in LEO, which indicates that the observed differences between LDEF and HST FEP might be attributed to the different soft x-ray fluences during these two missions.

## INTRODUCTION

Teflon<sup>®</sup> FEP is commonly used on exterior spacecraft surfaces in the LEO environment for thermal control. Silverized or aluminized FEP (Ag-FEP and Al-FEP, respectively) is used for the outer layer of thermal control blankets because of the low solar absorptance ( $\alpha_s = 0.08$  and  $0.13$ , respectively) and high thermal emittance ( $\epsilon = 0.81$  and  $0.81$  respectively) of these materials.<sup>1</sup> These optical properties provide very low solar absorptance to thermal emittance ratios ( $\alpha_s/\epsilon = 0.10$  and  $0.16$ , respectively) which are required for maintaining spacecraft temperatures in LEO. FEP is also preferred over other spacecraft polymers because of its relatively high resistance to atomic oxygen erosion. Based on shuttle flight experiments, the erosion yield of Kapton in LEO is  $3.0 \times 10^{-24}$  cm<sup>3</sup>/atom, while that of FEP was found to be  $0.037 \times 10^{-24}$  cm<sup>3</sup>/atom.<sup>2</sup> Because of its comparably low atomic oxygen erosion yield, FEP has been used unprotected in the space environment. Recent, long term space exposures such as on the Long Duration Exposure Facility and the

Hubble Space Telescope have provided evidence of LEO environmental degradation of FEP. The erosion yield of FEP, for example, has been found to be  $0.34 \times 10^{-24} \text{ cm}^3/\text{atom}$  based on LDEF data, an order of magnitude higher than determined from short term exposures.<sup>3,4</sup>

LDEF was a large ( $\approx 30$  ft. long and 14 ft. diameter) cylindrically shaped free-flying long-term space exposure satellite. LDEF had 12 sides (rows 1-12), each containing 7 experiment trays (A-F), and space and earth facing ends. LDEF was launched in April, 1984 with an orbital altitude of 482 km (28.5 degree inclination) and retrieved in January, 1990 at an altitude of 340 km after 5.8 years in space.<sup>5</sup> LDEF traveled with a fixed orientation such that row 9 (the leading edge) faced approximately into the ram direction, and row 3 (the trailing edge) was in the wake direction. Row 9, which was exposed to almost normal ( $8.1^\circ$  yaw offset) directed ram atomic oxygen (AO), received an AO fluence of  $8.99 \times 10^{21}$  atoms/cm<sup>2</sup>, while row 3 had received very little AO ( $1.32 \times 10^{17}$  atoms/cm<sup>2</sup>).<sup>5</sup> Row 4 experienced the lowest AO fluence of  $2.31 \times 10^5$  atoms/cm<sup>2</sup>. The solar exposures for the leading and trailing edges were essentially the same (11,156 and 11,110 equivalent sun hours (ESH), respectively)<sup>6</sup> providing a large variation in the AO/solar exposure ratios for the LDEF rows. LDEF had a total of 57 experiments on it. Two of the experiments, A0178 and P0004, were covered with silvered Teflon thermal control blankets. P0004 was located on row 2 (F-2). Experiment A0178, the cosmic-ray experiment, consisted of 16 trays located on 9 different rows around LDEF, exposing Ag-FEP to a wide variety of environmental exposures.<sup>5</sup>

The Hubble Space Telescope was launched in April 1990 with an orbital altitude of 614 km (28.5 degree inclination). The telescope was designed to be serviced in space, and the first servicing mission was in December 1993. At the time of the first servicing mission, HST was at an altitude of 587 km and had operated in the LEO space environment for 3.6 years. A large portion of the exterior of HST is covered with MLI thermal control blankets. Depending on the location, the outer-most layer of these blankets is either Al-FEP or Ag-FEP. Both types of FEP MLI were retrieved by the astronauts during the first servicing mission.

During HST's first servicing mission, two new magnetic sensing systems (MSS) were placed on top of the old ones. Al-FEP thermal control blankets covering the original MSS electronics boxes were removed during servicing and brought back to Earth. The five sides of the MSS MLI blankets received varying solar exposures from 4,477 to 16,670 ESH.<sup>3</sup> The solar arrays, which were built by the European Space Agency (ESA), were replaced with new arrays during the first servicing mission. One of the two replaced arrays was retrieved and brought back to Earth. The second array was jettisoned into space because it could not be retracted. The solar array drive arm (SADA) of the retrieved array was covered with Ag-FEP MLI. This FEP blanket material had solar and anti-solar facing sides with 20,056 and 6,260 ESH exposures, respectively.<sup>7</sup> A piece of the Ag-FEP MLI material from the retrieved solar array was made available by ESA for evaluation.

Samples of FEP from LDEF and HST have been evaluated for solar induced embrittlement and for synergistic effects of solar degradation and atomic oxygen. Surface hardness and depth of embrittlement are compared. These exposures provide unique opportunities for studying environmental degradation because of the long durations and the different conditions (such as differences in altitude, orientation, etc.) of the exposures. Soft x-ray testing was conducted and compared to tensile results to help understand the degradation mechanisms of FEP in the LEO environment.

## MATERIALS AND EXPERIMENTAL PROCEDURES

### Materials & Exposures

**LDEF FEP.** The Ag-FEP thermal control blankets used on LDEF experiments A0178 and P0004 consists of 5 mil (127  $\mu\text{m}$ ) FEP with  $\approx 800 \text{ \AA}$  of vapor deposited silver on the backside and  $400 \text{ \AA}$  of vapor-deposited Inconel on top of the silver. A 2-3 mil coating of black Chemglaze Z306 polyurethane based paint was sprayed onto the Inconel.<sup>5</sup> Samples of LDEF Ag-FEP from these two experiments, which were provided to NASA Lewis Research Center (LeRC) for evaluation, are listed in Table 1, along with their environmental exposures.<sup>5,6,8</sup> A LDEF ground control sample was also provided for comparison.

**HST MSS FEP.** The outer most layer of the retrieved HST MSS MLI is 5 mil FEP with vapor deposited aluminum (VDA) on the backside. Underneath the Al-FEP layer are layers of embossed Kapton with VDA on both sides. The MLI blanket is held together in selective areas with acrylic adhesive and stitching. Figure 1 shows the two retrieved magnetometer MLI cover assemblies. The blankets are approximately 35 x 38 cm in size. The two holes in the blankets are for cable access and are on the side of the blankets which received the highest solar exposure. Figure 1b is a close-up of one of the cable holes. Figure 2 is a sketch of the sample locations along with calculated solar exposures for the 5 “sides” of the blanket.<sup>9</sup> Table 2 summarizes the HST MSS samples and their environmental exposures. The two magnetometers received identical but symmetrical solar exposures. Because the MSS blankets are identical, and unlabeled, it was not known which blanket was on which MSS electronics box. Therefore, it was not known which of the two sides received 6,324 ESH (+V1 direction) or 9,193 ESH (-V1 direction). An atomic oxygen ram fluence of  $4.9 \times 10^{20}$  atoms/cm<sup>2</sup> for the mission duration has been calculated at NASA Goddard Space Flight Center (GSFC) using the Mass Spectrometer Incoherent Scatter Model (MSIS-86). Because of the random positioning of the MSS with respect to the ram direction, the AO fluence was estimated to be  $1/\pi$  of the ram fluence ( $1.56 \times 10^{20}$  atoms/cm<sup>2</sup>) for the side of the MSS blanket facing directly out to space (side D), and  $1/2\pi$  of the ram fluence ( $7.8 \times 10^{19}$  atoms/cm<sup>2</sup>) for the 4 sides of the MSS which have a view of the telescope and are therefore shielded from AO during a portion of the orbit. Scattering contributions have not been included in the atomic oxygen fluences.

**HST SADA FEP.** The SADA MLI provided by ESA has an outer layer of 5 mil FEP coated on the backside with Ag and then Inconel (1600 Å). An acrylic adhesive was used to bond a glass fiber cloth impregnated with PTFE to the Inconel. Below this outer layer are 16 layers of double-sided VDA on 2 mil Kapton separated by Dacron net. The bottom layer is glass fiber cloth impregnated with PTFE. The SADA MLI blanket was held together with stitching and contained vent holes. The blanket was wrapped around the circumference of the drive arm assembly and the adjoining edges were stitched to hold the blanket in place. There were four separate sections of MLI which covered the SADA, and the section closest to the body of HST was removed by ESA, cut in half and provided for analyses. ESA cut the SADA MLI such that both solar and anti-solar facing surfaces were available. See Figure 3 for a sketch of the SADA MLI and for sample positioning.

Solar fluences were calculated by ESA for the solar and anti-solar facing solar array surfaces were calculated by Drolshagen.<sup>7</sup> Because of differences in the calculated ram AO fluences from the MSIS data and Drolshagen’s model, the SADA AO fluence values were estimated based on the ram fluence calculated from the MSIS-86 program so the values would be consistent with the MSS values. The MSIS-86 ram fluence was multiplied by the solar-to-ram facing atomic oxygen flux ratio (0.2528) for Space Station to estimate the solar facing AO fluence. This value was then divided by 2 for a fluence of  $6.18 \times 10^{19}$  atoms/cm<sup>2</sup> to account for periods of shadowing. The anti-solar fluence was calculated similarly using the anti-solar-to-ram ratio (0.3167) for Space Station, then divided by 2 to get an anti-solar facing AO fluence of  $7.76 \times 10^{19}$  atoms/cm<sup>2</sup>. Scattering contributions have not been included in the atomic oxygen fluences. The environmental exposures for the solar facing sample (31) and anti-solar facing sample (38) are listed in Table 2. There are no fluence data for samples 32-37.

### Experimental Procedures

**Surface Hardness.** Surface hardness was determined by micro-indenter measurements at Nano Instruments, Inc. using a NANO INDENTER<sup>®</sup>II, Mechanical Properties Microprobe (MPM). The MPM performs ultra-low-load indentations using a diamond indenter tip of known geometry with the load and displacement (i.e. depth of indentation) continuously monitored. Using a continuous stiffness measurement (CSM) technique, hardness versus depth can be determined during a single indentation event. This technique enables the determination of surface hardness versus depth for soft materials, such as polymers, in addition to metals. Hardness was determined on LDEF, HST and pristine material from 5-500 nm depth at approximately 5 nm intervals. Up to 180 data points were obtained and averaged at each depth, with more data points being averaged near the surface.

**Bend Testing.** Samples approximately 0.5 x 2.0 cm were subject to bend testing to evaluate surface cracking. The samples were bent around a 0.83 mm diameter mandrel with the exposed FEP surface in tension. This corresponds to

an induced strain of 13.3% for 5 mil thick samples. Each sample was exposed to 25 bend cycles. The area which was bent was examined prior to, and after bending with an Olympus Stereo-zoom optical microscope. Images were obtained between 12 to 101 magnification to look for tension induced surface crazing.

**Crack Depth Measurements.** Samples which were bend tested were cross-sectioned to enable crack depth measurements to be made. The samples were mounted in metallography epoxy on edge and polished using standard metallography techniques. Optical micrographs between 500-800x were taken of the cross-sectioned samples at the bend tested area. Crack depth measurements were obtained from micrographs and average crack depths were computed.

**Surface Morphologies.** Surface textures of the HST MSS samples were evaluated using a JEOL 840A scanning electron microscope (SEM) operated at an accelerating voltage of 15 kV. Samples were coated with a thin conductive layer of Au prior to examination. The surface topography of MSS samples 125 and 135 were obtained with a Park Scientific AutoProbe scanning probe microscope. Atomic force microscope (AFM) images were taken with 3 or 10  $\mu\text{m}$  image areas and compared to pristine FEP.

**Soft X-ray Exposure.** Soft x-ray testing was conducted on 2 mil pristine FEP in an electron beam facility. An aluminum target was irradiated with a 9.51 keV electron beam. The base pressure of the system during exposure was approximately  $1 \times 10^{-6}$  torr. A 2  $\mu\text{m}$  thick Al foil barrier was used to help reduce electron irradiation from the target. Unmonochromatic Al  $K_{\alpha}$  x-rays were produced and have an energy peak at 1.49 keV ( $\lambda$  of 8.34  $\text{\AA}$ ). Rectangular samples were irradiated for 5 hours for bend testing, and "dog-bone" samples were irradiated for tensile testing. Two samples were irradiated at a time, and due to facility geometry one sample received a higher x-ray dose than the other. The x-ray flux has not yet been characterized for the facility.

**Tensile Testing.** Tensile testing was conducted at NASA GSFC on the MSS MLI<sup>3</sup> and at NASA LeRC on pristine material and soft x-ray exposed material. Testing was conducted in accordance with ASTM D1822 Type L at GSFC and in accordance with ASTM D368 Type V at LeRC. The only MSS material tested was from section D (11,339 ESH) because of the size and configuration of other sections. The SADA material was not tested because it was bonded to a composite cloth. LDEF samples had been previously tensile tested by Boeing<sup>5</sup> and others.

## RESULTS AND DISCUSSION

**Visual Examination.** The solar facing HST FEP appeared to be significantly more structurally damaged after 3.6 years in LEO than the LDEF FEP after 5.8 years in LEO. The MSS MLI FEP was obviously embrittled, with cracking of the FEP observed on the higher solar exposure sides of the MLI blanket, as seen in Figure 4a. Solar induced FEP degradation has been attributed to photodissociation of carbon-carbon bonds through chain scission and breaking of carbon-fluorine bonds. Further photodissociation causes double-bond formation, radical formation and cross-linking. A highly cross-linked surface layer results in surface embrittlement.<sup>10,11</sup> Through-thickness cracking of the FEP was observed around the cable holes (see Figure 4b) along with FEP delamination from the aluminized layer. The MSS blankets were attached with Velcro<sup>®</sup>, therefore the astronauts had to manipulate them to remove them. They were then packed into plastic bags for transport. The majority of observed cracks in the MSS MLI were likely to have been introduced during retrieval handling. No visible cracks were observed in the FEP from the side with the lowest solar exposure. The SADA MLI was retrieved and examined in its operational state. The blanket received no on-orbit handling, yet on solar facing surfaces, adjacent to stitched areas or vent holes, through-thickness cracks were observed in the 5 mil FEP (see Figure 5). More details of the condition of the as-retrieved HST materials are available elsewhere.<sup>3</sup>

No visible cracks were observed on any of the LDEF samples. There was, however, a striking difference in the appearance of the leading and trailing edge samples. The leading edge samples had a white, diffuse appearance and the trailing edge samples looked pristine (shiny and reflective). The hazy appearance of the leading edge FEP is due to the well documented, cone-like carpet morphology developed by directed ram atomic oxygen erosion texturing.<sup>4,12</sup> These cones are approximately 2  $\mu\text{m}$  in height for FEP from LDEF row 10, as can be seen in Figure 6a.<sup>4</sup> The HST samples did not appear hazy, although some areas were notably darkened. Scanning electron microscopy examination of the high solar fluence HST MSS samples revealed a roughened surface morphology compared to low solar fluence samples, as seen in Figure 6b and 6c, respectively. Because these samples received the same AO fluences, a synergistic texturing

effect has occurred with solar fluence. AFM analysis indicated the roughness of MSS sample 127 (16,670 ESH) to be approximately 0.2  $\mu\text{m}$  in height, an order of magnitude less than the LDEF leading edge texture, but an order of magnitude higher than for pristine FEP. MSS FEP should not develop a cone-like morphology because the ram AO arrival direction varied over time.

Because of the apparent severity of FEP embrittlement of the HST samples, as compared to the longer LEO exposed LDEF samples, tests were conducted to quantify the extent of embrittlement of FEP for both environments.

**Surface Hardness.** Surface hardness results versus depth for the LDEF samples are shown in Figure 7. This unique hardness measurement technique was able to detect an increased surface hardness for samples from the trailing edge. Also, there seems to be a trend for increasing hardness with decreasing AO/solar fluence ratio. This is attributed to a competing interaction of AO erosion and solar radiation induced embrittlement. The only samples which did not follow this trend are those from row 4. These samples appeared cloudy (particularly sample A-04) unlike the rest of the trailing edge samples. These cloudy areas have been attributed to silicon contamination.<sup>13</sup> Samples C-08, E-10 and D-11 which are highly textured, appear softer than the control sample. This is probably an artifact of the sampling technique. It is likely that bending over of the very soft, atomic oxygen textured surface cones made these samples appear softer than the control. For these highly textured samples, more accurate hardness values may be obtained on cross-sectioned samples. Although values at the surface would not be able to be obtained.

Figure 8 is a graph of the average hardness versus depth for the HST samples. Surface embrittlement is observed for all of these samples. The HST MSS samples do not follow a trend for decreasing hardness with increasing AO/solar fluence ratios at the very surface of the samples (15 nm), but appear to at depths >100 nm. There seems to be a trend for increasing hardness with increasing solar fluence, but with the data points at 6,324 ESH (sample 128) and 9,193 ESH (sample 130) possibly switched, this can not currently be verified. Also, sample 134 (4,477 ESH) appears to have a higher surface hardness than expected. This sample's hardness decreases versus depth at a much faster rate than for the other samples, which indicates that there may be other factors contributing to the surface hardness, such as contamination. Based on the hardness data, an AO fluence of  $7.8 \times 10^{19}$  atoms/cm<sup>2</sup> in the HST environment was not sufficient to remove the embrittled layer from solar exposure of 6,324 ESH. This corresponds to an erosion depth of 0.27  $\mu\text{m}$ , based on LDEF FEP erosion yield data.<sup>2</sup>

When comparing the LDEF and HST data, for equivalent AO/solar fluence ratios (this ratio is used as a means to compare exposures for these two missions), the HST samples seem significantly harder than the LDEF samples. This can be seen in Figure 9a which shows the hardness at a depth of 15 nm versus AO/solar fluence for both LDEF and HST samples. Yet, if one compares the hardness versus solar fluence for both the LDEF and HST samples, the HST samples are not necessarily harder than the LDEF samples, as can be seen in Figure 9b. These comparisons are further complicated due to the high AO fluence variations between the different samples on LDEF. The AO fluence dominates the AO/solar fluence ratio curve, while the AO is completely ignored in the solar fluence curve. Also, care needs to be taken when comparing data based on AO/solar fluence ratios. Different effects are likely for high fluence exposures and low fluence exposures, both of which can produce the same ratio.

**Bend Testing and Crack Depth Measurements.** Results of bend testing and crack depth measurements are listed in Tables 3-5. Figure 10 shows the surface of SADA sample 31 prior to, and after, bend testing. These parallel cracks are typical of the kind of surface cracking which occurred for LEO embrittled FEP with bend testing. LDEF samples with a high AO/solar fluence ratio ( $\geq 4 \times 10^{17}$ ) ratio did not crack in tension when bent around an 0.83 mm diameter mandrel. These results are consistent with the surface hardness data. The samples which are softer than the LDEF control (E-10, D-11, C-08), and sample D-07, which appears similar in hardness at the surface of the sample as the control (the 5 nm control data was unfortunately not obtained), do not have embrittled surfaces as measured by either surface hardness or bend testing. The LDEF data shows that samples with an AO fluence  $>8 \times 10^{21}$  atoms/cm<sup>2</sup> received a high enough AO flux to remove, or prevent formation of, an embrittled layer induced by solar exposure of 10,700 ESH. This corresponds to an erosion depth of 27.2  $\mu\text{m}$ . A fluence of  $5 \times 10^{19}$  atoms/cm<sup>2</sup> (erosion depth of 0.17  $\mu\text{m}$ ) did not completely remove the embrittled layer induced by 6,438 ESH. This is consistent with the HST data reported above which showed an embrittled layer induced by 6,324 ESH remained after an erosion of 0.27  $\mu\text{m}$ . It should be noted that the AO flux increased dramatically during the last year of the LDEF mission.

As expected, the HST samples with highest solar exposure cracked with bend testing. Even though hardness tests indicated an embrittled layer, samples exposed to low solar exposures (4,477 ESH) did not crack with bend testing. Although many of the MSS samples had as-received surface cracking, non-cracked areas were bend tested so that the depth of induced cracking for a particular strain would be compared with all samples. For samples with the greatest extent of surface erosion,<sup>3,4</sup> the bend test induced surface strains were 10.6% and 11.4%, for LDEF and HST, respectively. It should be noted that there was a cable bundle covering the SADA MLI, most likely over samples 35 and 36.

Figure 11 is a typical optical micrograph of a cross-sectioned sample (MSS 130) showing bend test-induced surface cracks. There seems to be a trend for increasing crack depth with decreasing AO/solar fluence for the LDEF samples. The average crack depth for the HST samples both increases with increasing solar fluence, and with decreasing AO/solar fluence ratio, as would be expected because the atomic oxygen fluence is so uniform. This is most obviously displayed if the deepest induced crack is plotted, as seen in Figure 12a and 12b, respectively.

When comparing the LDEF and HST crack depth data, the HST samples appear more damaged if the AO/solar fluence ratios are compared. Figure 13a shows significantly deeper cracks in most of the HST samples than for the LDEF samples. When comparing the deepest induced crack versus solar fluence for the LDEF and HST samples, as seen in Figure 13b, again, the HST samples do appear embrittled deeper than the LDEF samples. In Figure 13b, it also becomes more obvious that the very deep cracks have received a higher solar fluence. The deepest HST crack was 5 times as deep as the deepest LDEF crack, for 2.5 times the solar fluence. It is not currently understood why the hardness data does not indicate an embrittled layer deeper than 500 nm, which does not correspond with the depth of embrittlement based on crack depth data. Hardness versus depth on cross-sectioned samples may provide some insight.

It is interesting that, although through-thickness surface cracking was observed on the as-retrieved HST samples, bend testing did not produce any through-thickness surface cracking. Because the areas which had through thickness cracks were in stressed areas, there may be a stress-corrosion type failure occurring on-orbit. It is also likely that thermal cycling played a role in the on-orbit cracking. Temperature fluctuations of -100 to +50°C are expected on solar facing Al-FEP surfaces on HST.

**Soft x-ray Exposure.** Ground tests were performed at LeRC on the AO and vacuum ultraviolet (VUV) radiation durability of Al-FEP for use as thermal shield material on HST solar array bi-stem booms. Samples were exposed up to 17,000 ESH of VUV and  $1.33 \times 10^{20}$  atoms/cm<sup>2</sup> of atomic oxygen. Although testing indicated the build-up of a VUV induced embrittled layer (as determined by surface hardness) for the expected mission AO/VUV fluence ratio, testing did not predict the severity of embrittlement witnessed in the HST environment on solar facing surfaces. Also, because the HST samples appear to be more embrittled than LDEF samples (based on the crack depth data), other environmental factors than the competing effects of atomic oxygen and solar fluence need to be assessed, which could contribute to FEP degradation in the HST LEO environment. One possible explanation is the increased dose of soft x-rays witnessed by HST as compared to LDEF due to variations in the frequency and fluence of solar flares for the two missions.<sup>14</sup> To help determine if soft x-rays play a role in the degradation of FEP in LEO, pristine 2 mil FEP was exposed to soft x-rays.

Soft x-ray irradiation produced similar surface cracking during bend testing as witnessed on the LEO samples (see Figure 14). Tensile tests show a decrease in the ultimate tensile strength with x-ray exposure, but the most obvious change in mechanical properties is noted in the drastic reduction in elongation for the exposed samples. The percent elongation at ultimate yield (as measured from the grip distance) for the soft x-ray exposed samples decreased from  $168 \pm 28\%$  to 66% and 32% for lower and higher flux x-ray exposed samples, respectively. This is a decrease in percent elongation from pristine FEP of 40% and 20%, respectively. These results are similar to those obtained by ESA, which showed a 48% decrease from pristine after Mg K<sub>α</sub> exposure.<sup>15</sup> The MSS sample had a  $45 \pm 17\%$  elongation relative to pristine FEP.<sup>3</sup> LDEF sample F-04, with a similar solar fluence as the MSS sample (10,458 ESH compared to 11,339 ESH, respectively) had the same decrease in elongation compared to pristine FEP as the MSS sample (56%), but the AO fluence of the LDEF sample was insignificant ( $2.31 \times 10^5$  atoms/cm<sup>2</sup>).<sup>5</sup> If the percent elongation is compared to C-06 (73% elongation compared to pristine), which has the closest AO/solar fluence ratio, the HST sample appears more damaged. These results indicate that soft x-rays may be playing a role in the degradation mechanisms of FEP in the LEO environment.



In addition to evaluating the role of soft x-ray exposure, charged particle (electron/proton) radiation may also play a role in LEO degradation of FEP. Based on the samples retrieved from the HST first servicing mission, charged particles do not appear to be contributing significantly to FEP embrittlement because the HST embrittlement has been found to be very solar fluence dependent. These particles, also called Van Allen radiation, are trapped in the geomagnetic field and are not part of solar winds. The low solar fluence HST samples had no surfacing cracking, while the high solar fluence samples had through thickness cracking of the FEP. Another possible contributor to the degradation processes are thermal effects. Thermal cycling ranges may play an important role in increased embrittlement on solar facing surfaces. This is particularly true if surfaces darken from contaminants and/or radiation effects and cause increased solar absorptance and therefore increased temperatures to occur.<sup>3</sup> Increased temperatures are known to cause increased radiation damage rates to polymers.<sup>11</sup> Estimates of temperature ranges for the LDEF Ag-FEP, HST Al-FEP and HST Ag-FEP are 0 to +60°C, -100 to +50°C, and -100 to +100°C<sup>15</sup>, respectively. These estimates do not account for increased temperatures due to darkening of FEP on solar facing sides of HST. Because the temperature range experienced by HST FEP included a phase transition temperature range at -93 to -13°C (and 72 to 107°C for the Ag-FEP), it is possible that this may have contributed to increased embrittlement on HST compared to LDEF.<sup>16</sup>

## CONCLUSIONS

With initial examination, Al-FEP and Ag-FEP from HST, appeared more damaged than LDEF Ag-FEP. Therefore, testing was conducted to quantify embrittlement through hardness and crack depth studies. There appeared to be a trend for increased surface hardness and depth of embrittlement of the LDEF samples with decreasing AO/solar fluence ratios. The LDEF data showed that samples with an AO fluence  $>3 \times 10^{21}$  atoms/cm<sup>2</sup> received enough AO to remove, or prevent formation of, an embrittled layer induced by solar exposure of up to 10,700 ESH. An AO fluence of  $5 \times 10^{19}$  atoms/cm<sup>2</sup> did not remove the embrittled layer induced by 6,438 ESH on LDEF. For HST, the damage to the FEP was found to increase directly with the solar fluence. An AO/solar fluence synergistic effect was observed for the HST FEP based on erosion morphology differences. The AO flux in the HST environment is not high enough to remove solar induced damage from the surface of FEP. Consistent with LDEF data, an AO fluence of  $8 \times 10^{19}$  atoms/cm<sup>2</sup> did not completely remove an embrittled layer produced by 6,324 ESH exposure on HST.

AO/solar fluence ratios were used as a means to compare LDEF and HST data because of the competing processes of solar embrittlement and AO erosion. When HST and LDEF data are compared using AO/solar fluence ratios, HST appears to be significantly more damaged than LDEF. But solar facing HST received significantly higher solar fluences than the LDEF samples. Yet, when just comparing solar exposures (for low LDEF AO fluences), the HST samples had deeper induced surface cracking than LDEF samples. These results underscore the necessity to consider causes for FEP embrittlement in addition to direct solar exposure, and removal effects of AO, such as the possible role of soft x-ray radiation which is dependent on solar flares. These results also illustrate the difficulties of trying to compare material from different spacecraft missions and environmental exposures. FEP that was exposed to soft x-rays in a ground test facility showed similar embrittlement as occurred in LEO, which indicates that the observed differences between LDEF and HST FEP might be attributed to the different soft x-ray fluences during these two missions. Continued testing of these unique materials, and materials from HST's second and third servicing missions, will aid in better understanding the degrading processes in LEO and therefore help to develop better ground tests to simulate the LEO environment.

## ACKNOWLEDGMENTS

The authors would like to thank Barry Lucas at Nano Instruments, Inc. for the surface hardness data, Todd Leonhardt and Michael Miller at NYMA for cross-sectioning metallography, and Demetrios Papadopoulos at the University of Akron for tensile testing. The authors would also like to thank Tom Zuby and the HST Project Office at NASA GSFC for providing the HST MSS material, Lothar Gerlach at ESA for providing the HST SADA material, and Boeing for providing some of the LDEF samples.

## REFERENCES

1. Henninger, J. H., "Solar Absorptance and Thermal Emittance of Some Common Spacecraft Thermal-Control Coatings," NASA RP-1121, 1984.

2. Banks, B. A. and Rutledge, S. K., "Low Earth Orbit Atomic Oxygen Simulation for Materials Durability Evaluation," *Spacecraft Materials in Space Environment*, Toulouse, France, Sept. 6-9, 1988, 371-392.
3. Zuby, T. M., de Groh, K. K. and Smith, D. C., "Degradation of FEP Thermal Control Materials Returned from the Hubble Space Telescope," *ESA WPP-77*, 1995, 385-402; also NASA TM-104627.
4. Banks, B. A., Dever J. A., Gebauer, L. and Hill, C., "Atomic Oxygen Interactions with FEP Teflon and Silicones on LDEF," *NASA CP-3134*, Part 2, 1991, 801-815.
5. Pippin, H. G., "Analysis of Silverized Teflon Thermal Control Material Flown on the Long Duration Exposure Facility," *NASA CR-4663*, July 1995.
6. Bourassa, R. J. and Gillis, J. R., "Solar Exposure of LDEF Experiment Trays," *NASA CR-189554*, Feb. 1992.
7. Drolshagen, G. "Definition of the Space Environment for the HST Solar-Array 1," *ESA WPP-77*, 1995, 53-65.
8. Pippin, H. G., "Analysis of Materials Flown on the Long Duration Exposure Facility: Summary of Results of the Materials Special Investigation Group", *NASA CR-4664*, July 1995.
9. Hitch, T. "MSS Flux Analysis," Technical Note No. JT94-TN008, Jackson and Tull for NASA GSFC Code 730, May 27, 1994.
10. Brinza, D. E., Stiegman, A. E., Staszak, P. R., Laue E. G. and Liang, R. H., "VUV Radiation-Induced Degradation of FEP Teflon Aboard the LDEF," *NASA CP-3134*, Part 2, 1991, 817-829.
11. English, L. K., "How High-Energy Radiation Affects Polymers," *Materials Engineering*, Vol. 103, May 1986, 41-44.
12. de Groh, K. K., Banks B. A. and Smith, D. C., "Environmental Durability Issues for Solar Power Systems in Low Earth Orbit," *Solar Engineering* 1995, 2, ASME, 1995, 939-950; also NASA TM-106775.
13. Hemminger, C. S., Stuckey, W. K., and Uht, J. C., "Space Environment Effects on Silvered Teflon Thermal Control Surfaces," *NASA CP-3134*, Part 2, 1991, 831-845.
14. Milintchouk, A., Van Eesbeek, M. and Levadou, F., "Soft X-ray Radiation as a Factor in the Degradation of Spacecraft Materials," *ICPMSE-3*, Toronto, Canada, April 25-26, 1996.
15. Van Eesbeek, M., Levadou, F. and Milintchouk, A., "Investigation on FEP from PDM and Harness from HST-SA1," *ESA WPP-77*, 1995, 403-416.
16. Reed, R. P., Schramm, R. E., and Clark, A. F., "Mechanical, Thermal and Electrical Properties of Selected Polymers," *Cryogenics*, Feb. 1973, 67-82.

Table 1. LDEF Samples and their Environmental Exposures

LDEF Sample	AO Fluence (atoms/cm <sup>2</sup> ) <sup>5</sup>	Solar Exposure (ESH) <sup>6</sup>	% of ESH Due to Earth Reflection <sup>8</sup>	AO/Solar Ratio (atoms/cm <sup>2</sup> •ESH)
Control	-	-	-	-
A-04 & F-04	2.31 E 5	10,458	10	2.21 E 1
B-05 & D-05	9.60 E 12	8,155	12	1.18 E 9
F-02	1.54 E 17	9,572	10	1.61 E 13
D-01	2.92 E 17	7,437	14	3.93 E 13
C-06	4.94 E 19	6,438	16	7.67 E 15
B-07 & D-07	3.39 E 21	7,111	14	4.77 E 17
C-11 & D-11	5.61 E 21	8,525	12	6.58 E 17
C-08	7.15 E 21	9,409	11	7.60 E 17
A-10 & E-10	8.43 E 21	10,698	9	7.88 E 17

Table 2. HST Samples and their Environmental Exposures

HST Sample	AO Fluence (atoms/cm <sup>2</sup> )	Solar Exposure (ESH)	% of ESH Due to Earth Reflection	AO/Solar Ratio (atoms/cm <sup>2</sup> •ESH)
MSS 125,126 & 127	0.78 E 20	16,670	16	4.7 E 15
MSS 132 & 133	1.56 E 20	11,339	7	1.4 E 16
MSS 130 & 131	0.78 E 20	9,193 or 6,324	33 or 72	8.5 E 15 or 1.2 E 16
MSS 128 & 129	0.78 E 20	6,324 or 9,193	72 or 33	1.2 E 16 or 8.5 E 15
MSS 134 & 135	0.78 E 20	4,477	100	1.7 E 16
SADA 31	0.62 E 20	20,056	2	3.1 E 15
SADA 38	0.78 E 20	6,260	100	1.2 E 16

Table 3. Crack Depth Data for LDEF Samples

Sample	Solar Fluence (ESH)	AO Fluence (atoms/cm <sup>2</sup> )	AO/Solar Fluence (atoms/cm <sup>2</sup> •ESH)	Deepest Crack (µm)	Ave. Crack Depth (µm)
LDEF F-04	10,458	2.31 E 5	2.21 E 1	11.3	4.80
LDEF D-05	8,155	9.60 E 12	1.18 E 9	13.8	10.0
LDEF F-02	9,572	1.54 E 17	1.61 E 13	1.25	1.77
LDEF D-01	7,437	2.92 E 17	3.93 E 13	12.5	6.64
LDEF C-06	6,438	4.94 E 19	7.67 E 15	9.38	5.94
LDEF D-07	7,111	3.39 E 21	4.77 E 17	-	-
LDEF D-11	8,525	5.61 E 21	6.58 E 17	-	-
LDEF C-08	9,409	7.15 E 21	7.60 E 17	-	-
LDEF A-10	10,698	8.43 E 21	7.88 E 17	-	-

Table 4. Crack Depth Data for HST MSS Samples

Sample	Solar Fluence (ESH)	AO Fluence (atoms/cm <sup>2</sup> )	AO/Solar Fluence (atoms/cm <sup>2</sup> •ESH)	Deepest Crack (µm)	Ave. Crack Depth (µm)
MSS 126	16,670	0.78 E 20	4.7 E 15	33.3	11.2
MSS 127	16,670	0.78 E 20	4.7 E 15	62.5	23.0
MSS 132	11,339	1.56 E 20	1.4 E 16	40.0	17.7
MSS 133	11,339	1.56 E 20	1.4 E 16	5.00*	2.94
MSS 130	9,193 or 6,324	0.78 E 20	8.5 E 15 or 1.2 E 16	18.8	10.5
MSS 131	9,193 or 6,324	0.78 E 20	8.5 E 15 or 1.2 E 16	38.8	10.3
MSS128	6,324 or 9,193	0.78 E 20	1.2 E 16 or 8.5 E 15	-	-
MSS 129	6,324 or 9,193	0.78 E 20	1.2 E 16 or 8.5 E 15	5.33	5.0
MSS 134	4,477	0.78 E 20	1.7 E 16	-	-
MSS 135	4,477	0.78 E 20	1.7 E 16	-	-

\* Next to the 4,477 section

Table 5. Crack Depth Data for HST SADA Samples

Sample	Solar Fluence (ESH)	AO Fluence (atoms/cm <sup>2</sup> )	AO/Solar Fluence (atoms/cm <sup>2</sup> •ESH)	Deepest Crack (µm)	Ave. Crack Depth (µm)
SADA 31	20,056	0.62 E 20	3.1 E 15	72.5	24.0
SADA 32	no data	no data	no data	45.0	15.0
SADA 33	no data	no data	no data	17.5	10.1
SADA 34	no data	no data	no data	2.50	16.3
SADA 35	(covered)	(covered)	-	-	-
SADA 36	(covered)	(covered)	-	-	-
SADA 37	no data	no data	no data	-	-
SADA 38	6,260*	0.78 E 20	1.2 E 16	-	-

\* All albedo exposure

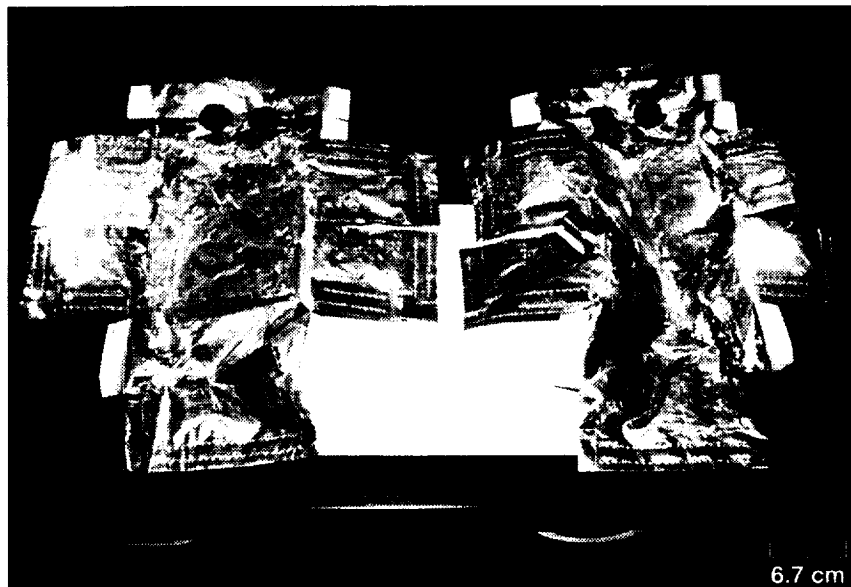


Figure 1. Retrieved HST Magnetometer MLI covers.

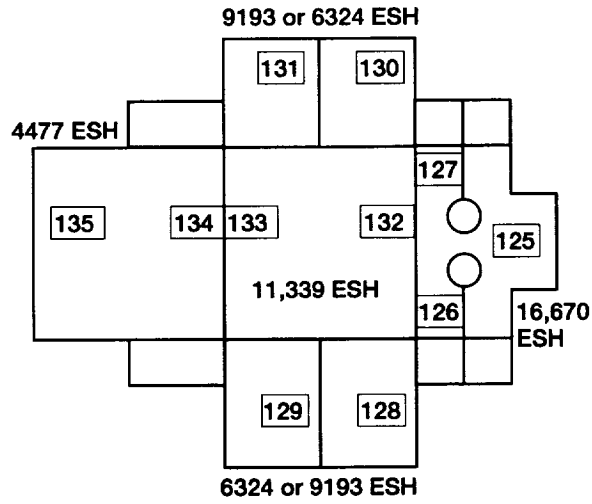


Figure 2. HST MSS MLI solar fluence and sample sectioning diagram.

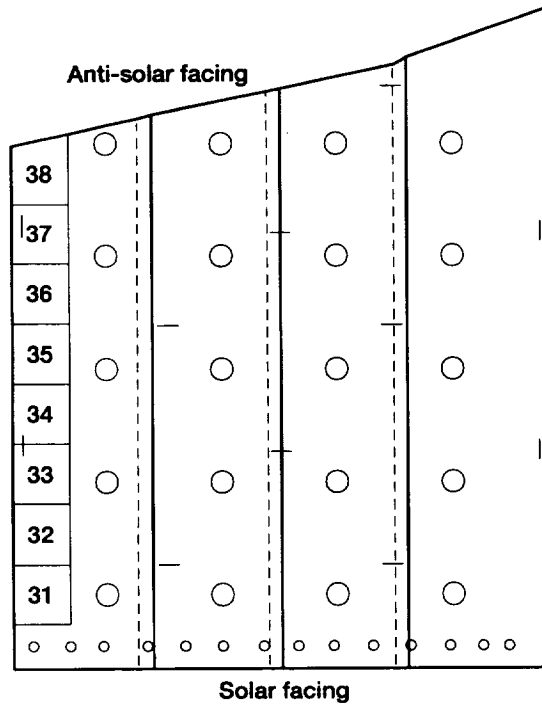


Figure 3. HST SADA MLI sample sectioning locations.

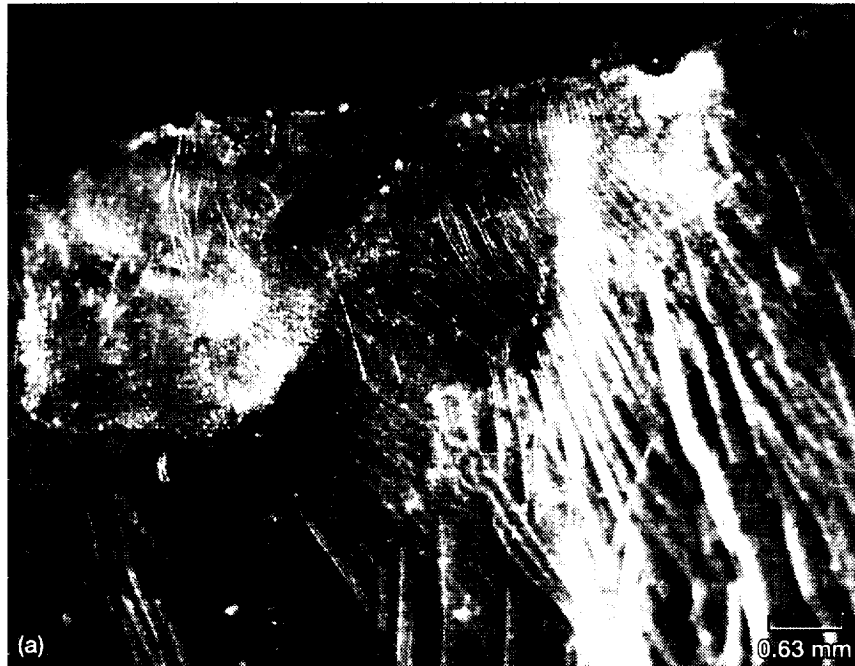


Figure 4. HST MSS MLI near cable holes (16,670 ESH). (a) Extensive cracking of FEP and delamination of FEP from Al (circular area on left). (b) Through thickness crack in 5 mil FEP.



**Figure 5. Through-thickness crack in the solar facing side of the HST SADA adjacent to a vent hole.**

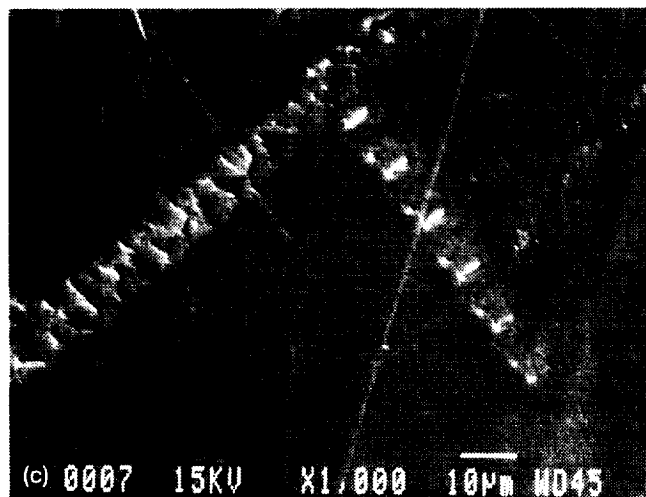
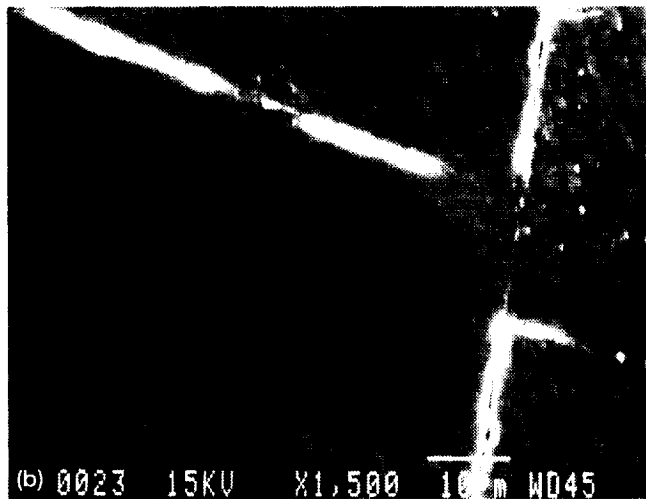
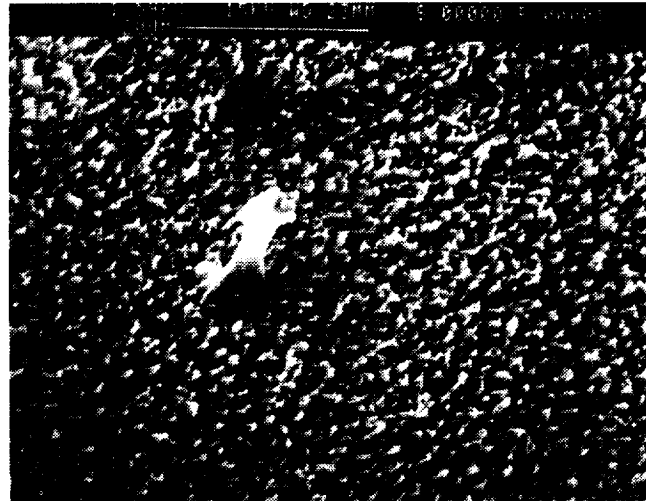


Figure 6. LEO erosion surface morphologies. (a) LDEP FEP from row 10 (10,698 ESH,  $8.43 \times 10^{21}$  atoms/cm<sup>2</sup>). (b) HST MSS sample 127 (16,670 ESH,  $7.8 \times 10^{19}$  atoms/cm<sup>2</sup>). (c) MSS sample 135 (4477 ESH,  $7.8 \times 10^{19}$  atoms/cm<sup>2</sup>).



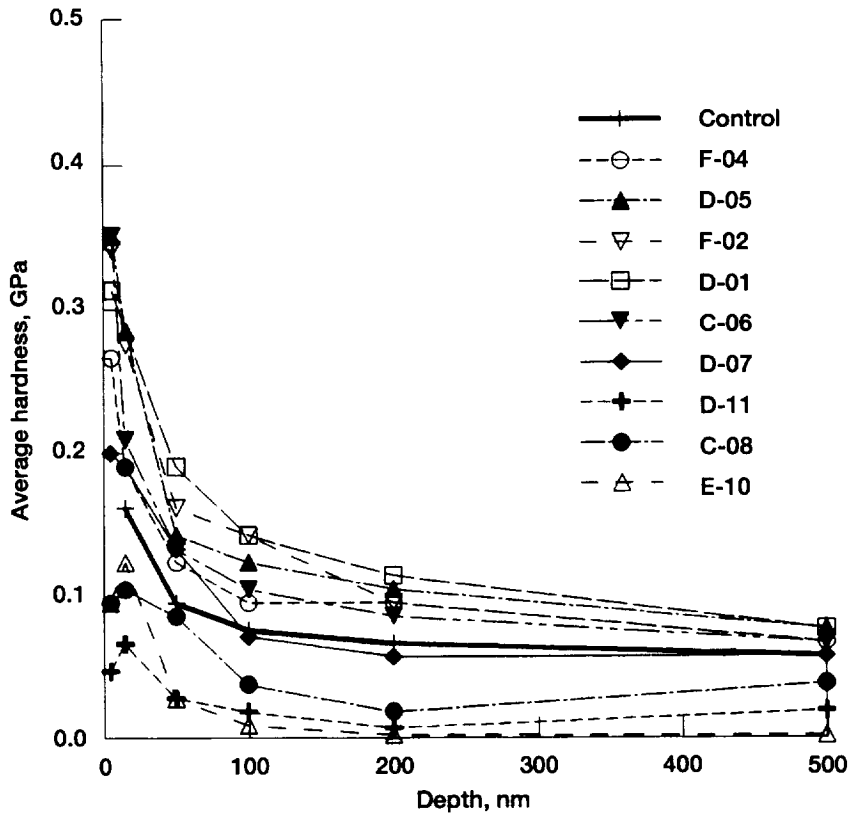


Figure 7. Average hardness versus depth for LDEF samples. Samples are listed in increasing AO/solar fluence ratios.

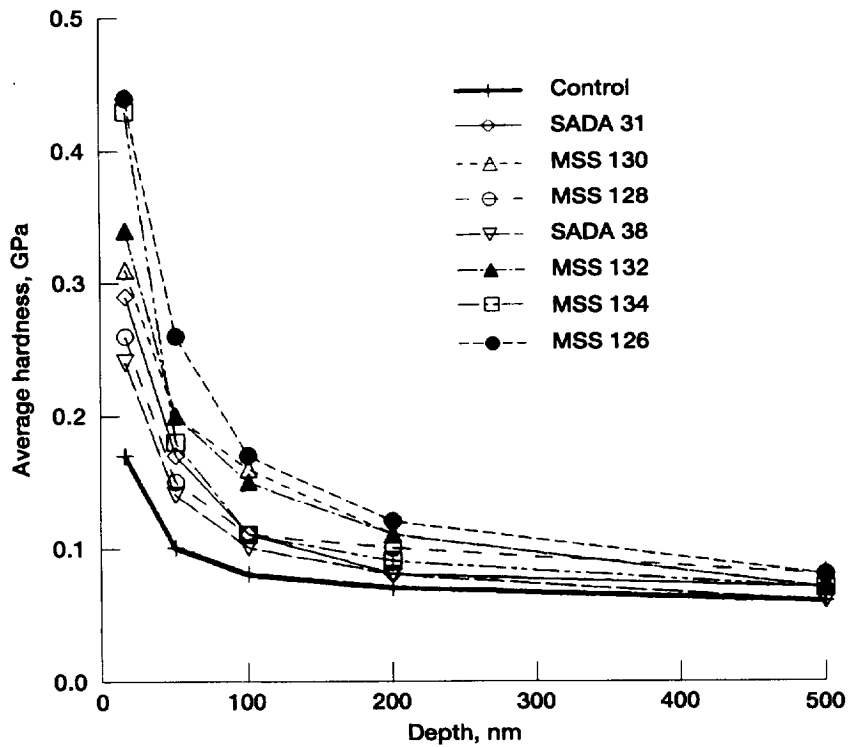


Figure 8. Average hardness versus depth for HST samples. Samples are listed in increasing AO/solar fluence ratios.

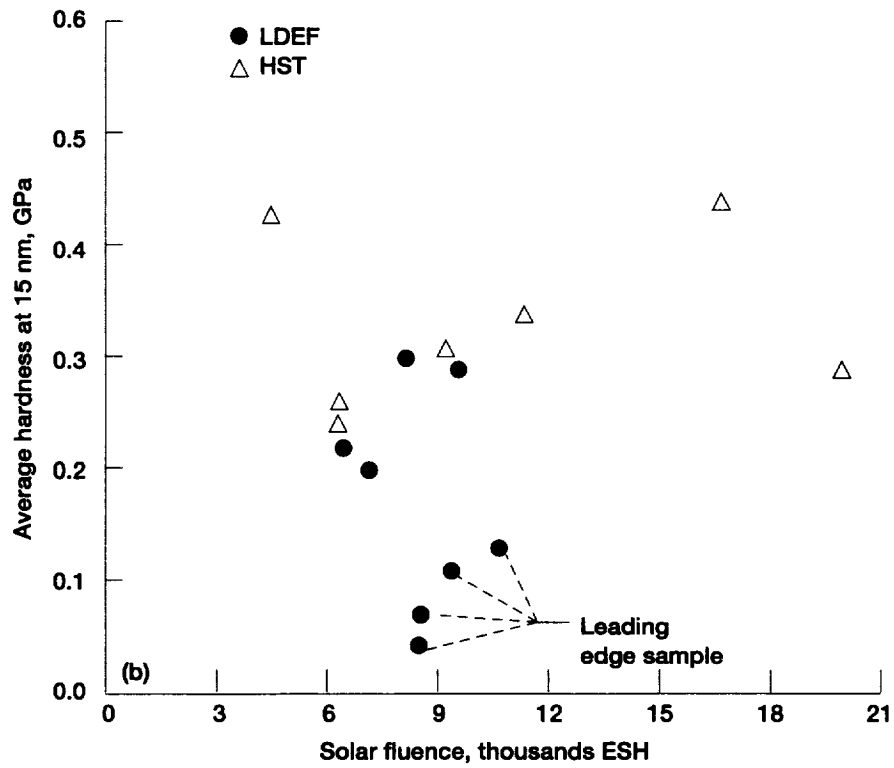
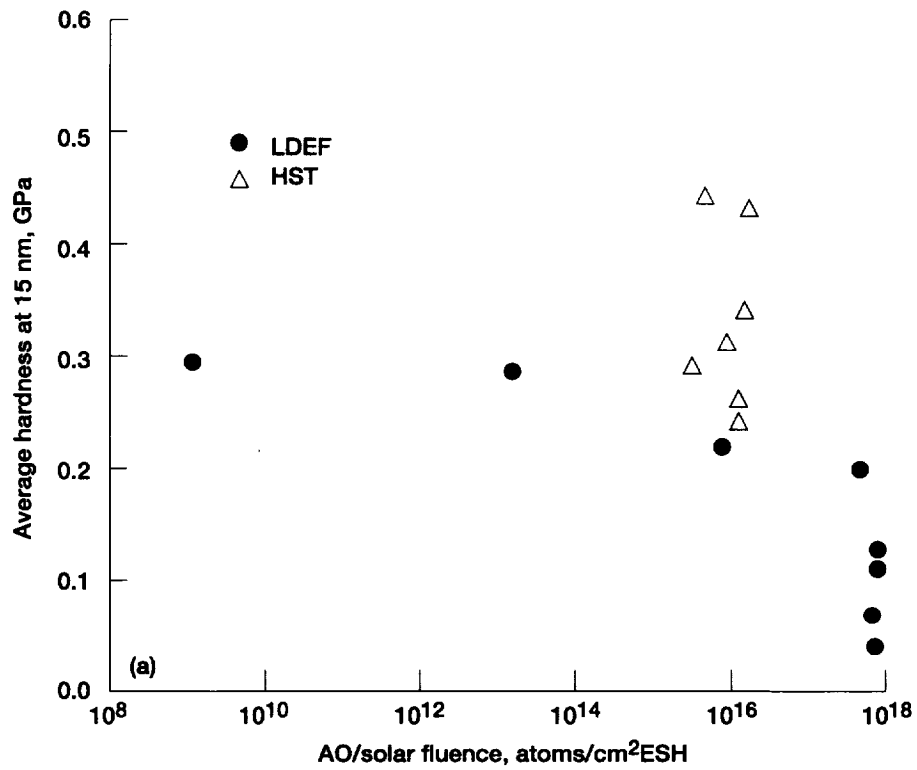


Figure 9. Average hardness at 15 nm depth for LDEF and HST samples. (a) Versus AO/solar fluence ratio. (b) Versus solar fluence.

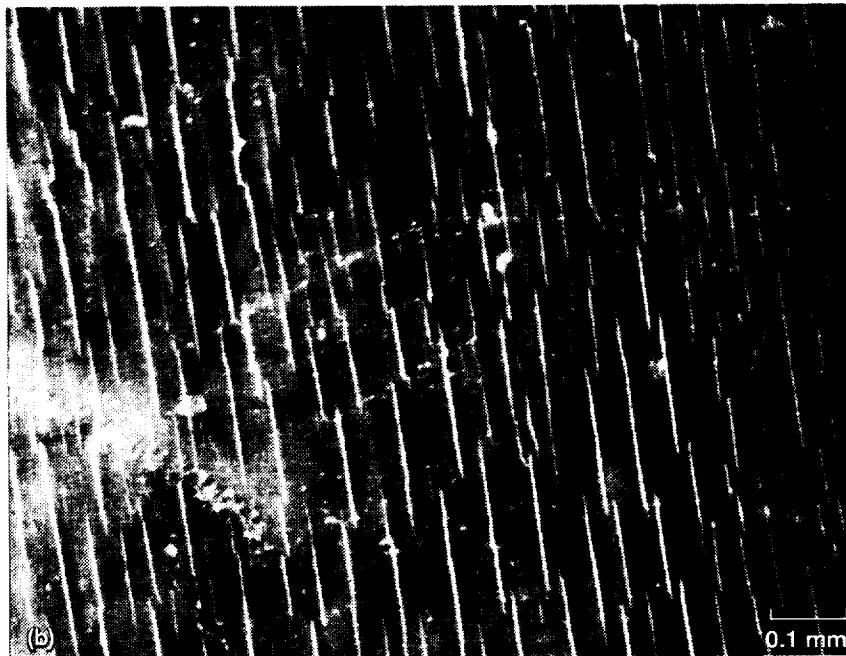
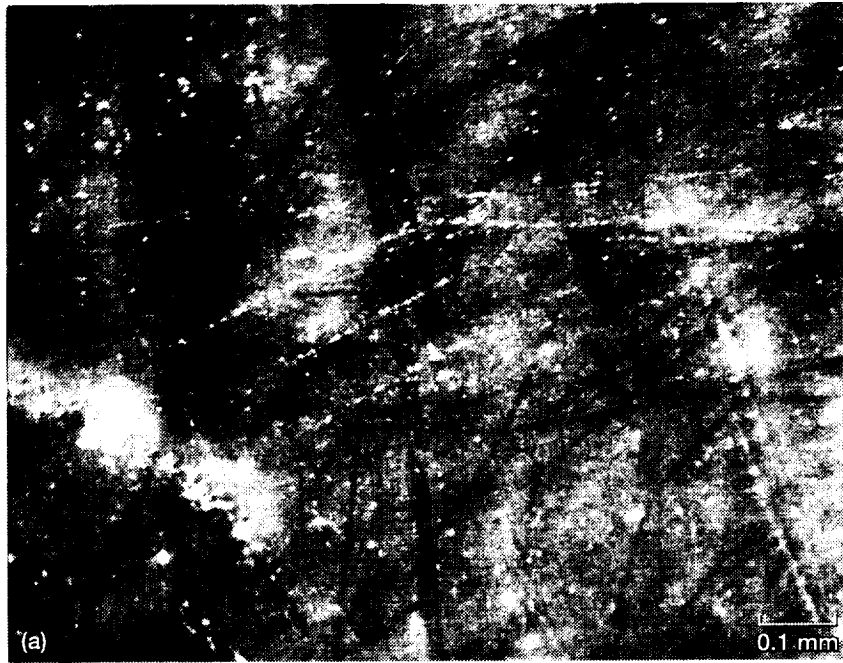
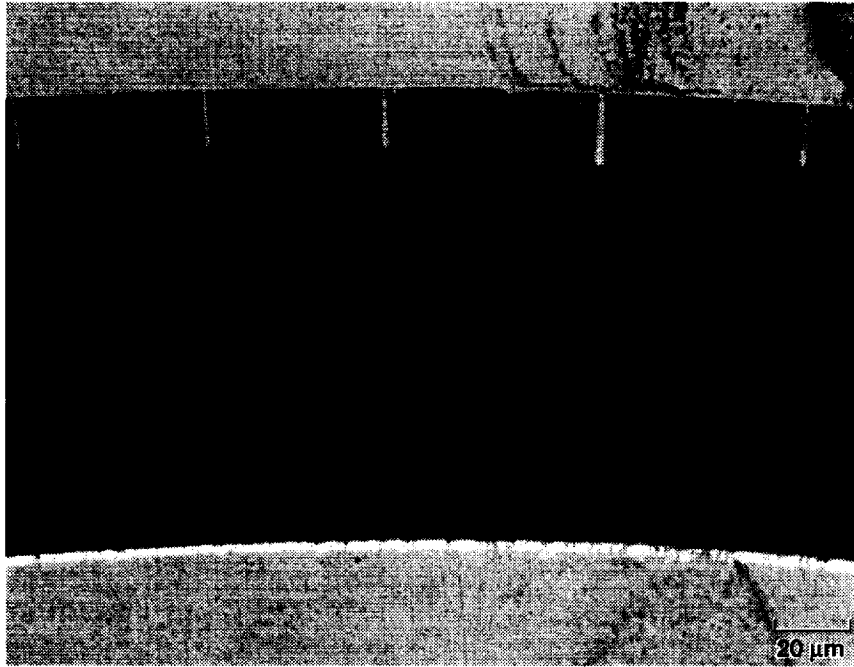


Figure 10. HST SADA sample 31 showing tension induced surface cracking. (a) Prior to bend testing. (b) After bend testing.



**Figure 11. Cross-sectioned view of bend test induced surface cracking in HST MSS sample 130.**

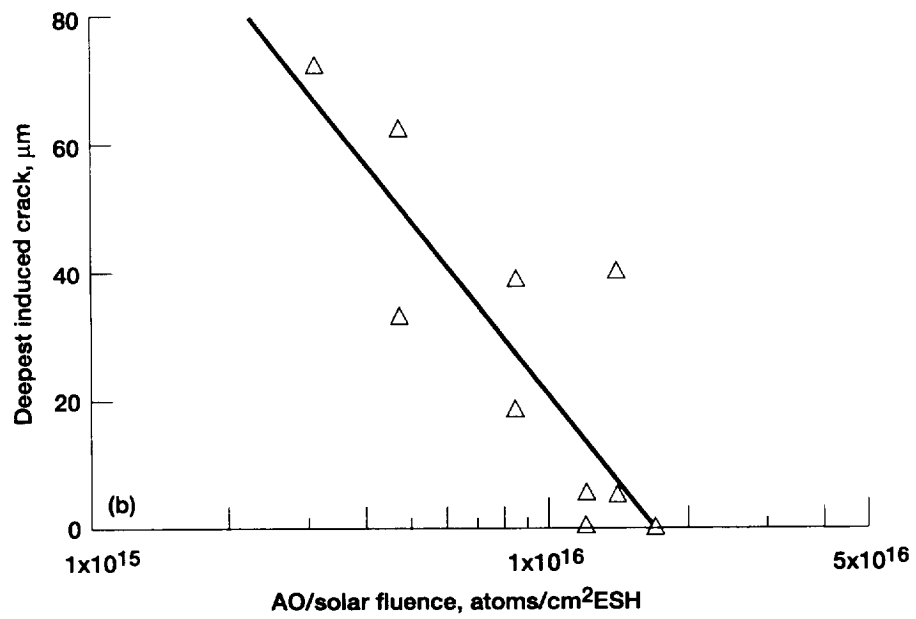
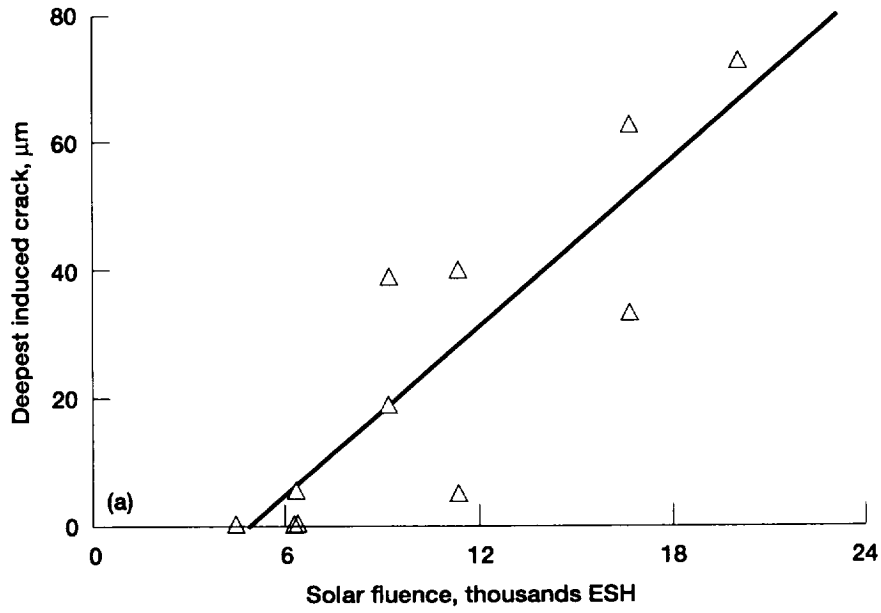


Figure 12. Deepest induced crack for HST samples. (a) Versus solar fluence. (b) Versus AO/solar fluence ratio.

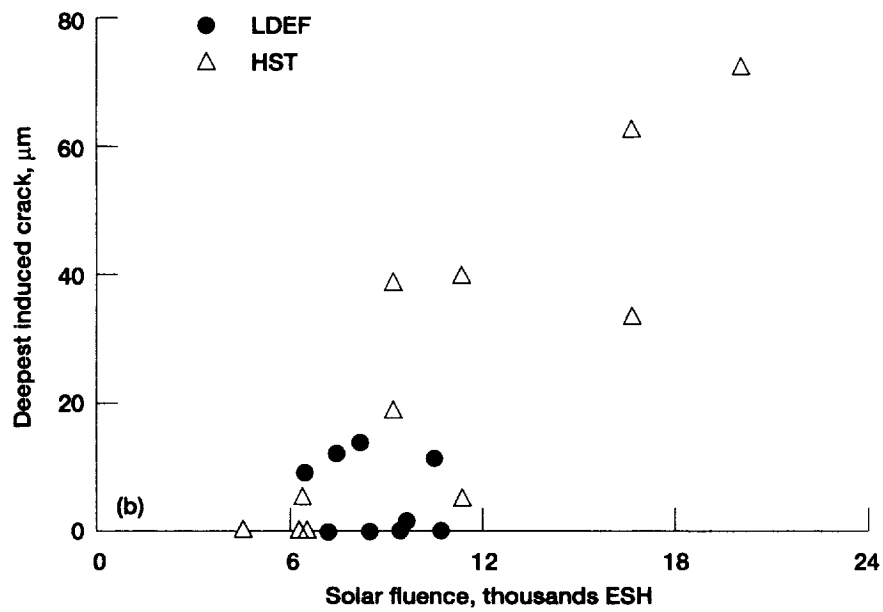
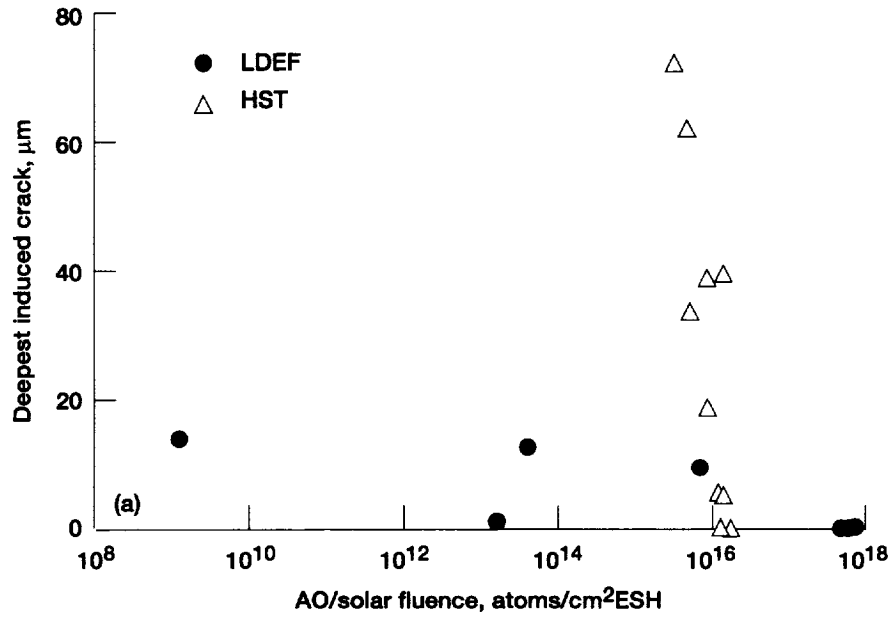


Figure 13. Deepest induced crack for LDEF and HST samples. (a) Versus AO/solar fluence ratio. (b) Versus solar fluence.

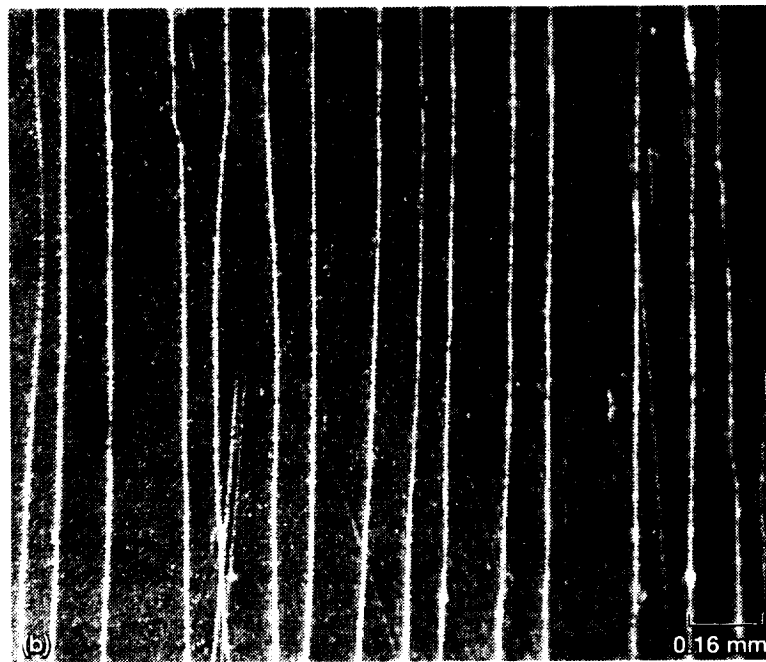
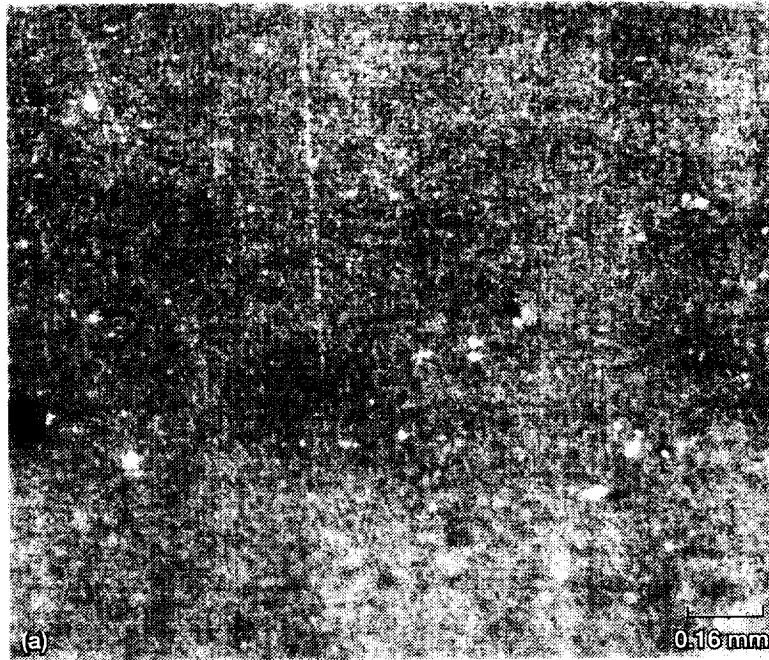


Figure 14. Soft x-ray exposed FEP showing bend test induced surface cracking. (a) Prior to bend testing. (b) After bend testing.

# REPORT DOCUMENTATION PAGE

*Form Approved*  
OMB No. 0704-0188

Public reporting burden for this collection of information is estimated to average 1 hour per response, including the time for reviewing instructions, searching existing data sources, gathering and maintaining the data needed, and completing and reviewing the collection of information. Send comments regarding this burden estimate or any other aspect of this collection of information, including suggestions for reducing this burden, to Washington Headquarters Services, Directorate for Information Operations and Reports, 1215 Jefferson Davis Highway, Suite 1204, Arlington, VA 22202-4302, and to the Office of Management and Budget, Paperwork Reduction Project (0704-0188), Washington, DC 20503.

<b>1. AGENCY USE ONLY (Leave blank)</b>		<b>2. REPORT DATE</b> December 1997	<b>3. REPORT TYPE AND DATES COVERED</b> Technical Memorandum	
<b>4. TITLE AND SUBTITLE</b>  Investigation of Teflon FEP Embrittlement on Spacecraft in Low Earth Orbit			<b>5. FUNDING NUMBERS</b>  WU-953-73-10-00	
<b>6. AUTHOR(S)</b>  Kim K. de Groh and Daniela C. Smith				
<b>7. PERFORMING ORGANIZATION NAME(S) AND ADDRESS(ES)</b>  National Aeronautics and Space Administration Lewis Research Center Cleveland, Ohio 44135-3191			<b>8. PERFORMING ORGANIZATION REPORT NUMBER</b>  E-10903	
<b>9. SPONSORING/MONITORING AGENCY NAME(S) AND ADDRESS(ES)</b>  National Aeronautics and Space Administration Washington, DC 20546-0001			<b>10. SPONSORING/MONITORING AGENCY REPORT NUMBER</b>  NASA TM-113153	
<b>11. SUPPLEMENTARY NOTES</b> Prepared for the Seventh International Symposium on Materials in a Space Environment cosponsored by the Centre d'Études et de Recherches de Toulouse (ONERA CERT), Agence Française de l'Espace (CNES), and the European Space Agency (ESA/ESTEC), Toulouse, France, June 16-20, 1997. Kim K. de Groh, NASA Lewis Research Center and Daniela C. Smith, Cleveland State University, 1983 E. 24th Street, Cleveland, Ohio 44115. Responsible person, Kim K. de Groh, organization code 5480, (216) 433-2297.				
<b>12a. DISTRIBUTION/AVAILABILITY STATEMENT</b>  Unclassified - Unlimited Subject Categories: 27, 18, and 92  This publication is available from the NASA Center for AeroSpace Information, (301) 621-0390.			<b>12b. DISTRIBUTION CODE</b>  Distribution: Nonstandard	
<b>13. ABSTRACT (Maximum 200 words)</b>  Teflon® FEP (fluorinated ethylene-propylene) is commonly used on exterior spacecraft surfaces in the low Earth orbit (LEO) environment for thermal control. Silverized or aluminized FEP is used for the outer layer of thermal control blankets because of its low solar absorptance and high thermal emittance. FEP is also preferred over other spacecraft polymers because of its relatively high resistance to atomic oxygen erosion. Because of this low atomic oxygen erosion yield, FEP has not been protected in the space environment. Recent, long term space exposures such as on the Long Duration Exposure Facility (LDEF, 5.8 years in space), and the Hubble Space Telescope (HST, after 3.6 years in space) have provided evidence of LEO environmental degradation of FEP. These exposures provide unique opportunities for studying environmental degradation because of the long durations and the different conditions (such as differences in altitude) of the exposures. Samples of FEP from LDEF and from HST (retrieved during its first servicing mission) have been evaluated for solar induced embrittlement and for synergistic effects of solar degradation and atomic oxygen. Micro-indenter results indicated that the surface hardness increased as the ratio of atomic oxygen fluence to solar fluence decreased for the LDEF samples. FEP multilayer insulation (MLI) retrieved from HST provided evidence of severe embrittlement on solar facing surfaces. Micro-indenter measurements indicated higher surface hardness values for these samples than LDEF samples, but the solar exposures were higher. Cracks induced during bend testing were significantly deeper for the HST samples with the highest solar exposure than for LDEF samples with similar atomic oxygen fluence to solar fluence ratios. If solar fluences are compared, the LDEF samples appear as damaged as HST samples, except that HST had deeper induced cracks. The results illustrate difficulties in comparing LEO exposed materials from different missions. Because the HST FEP appears more damaged than LDEF FEP based on depth of embrittlement, other causes for FEP embrittlement in addition to atomic oxygen and ultraviolet (UV) radiation, such as thermal effects and the possible role of soft x-ray radiation, need to be considered. FEP that was exposed to soft x-rays in a ground test facility, showed embrittlement similar to that witnessed in LEO, which indicates that the observed differences between LDEF and HST FEP might be attributed to the different soft x-ray fluences during these two missions.				
<b>14. SUBJECT TERMS</b>  Teflon FEP; LEO; Solar radiation; Atomic oxygen; LDEF; HST; Embrittlement			<b>15. NUMBER OF PAGES</b> 27	
			<b>16. PRICE CODE</b> A03	
<b>17. SECURITY CLASSIFICATION OF REPORT</b> Unclassified	<b>18. SECURITY CLASSIFICATION OF THIS PAGE</b> Unclassified	<b>19. SECURITY CLASSIFICATION OF ABSTRACT</b> Unclassified	<b>20. LIMITATION OF ABSTRACT</b>	